HYSTERESIS IN THE LORENZ EQUATIONS

A.C. FOWLER
Department of Mathematics, Massachusetts Institute of Technology, Cambridge, MA 02139, USA

and

M.J. McGUINNESS
Department of Applied Mathematics, California Institute of Technology, Pasadena, CA 91125, USA

Received 29 July 1982
Revised manuscript received 26 August 1982

The phenomenon of hysteresis, associated with multiple stable solution behaviours, has been predicted and observed in the Lorenz equations when r and σ are large.

1. Much of the recent literature on chaos in dynamical systems has been concerned with pointing out the behavioural similarity of many different types of models. The transition to aperiodic motion via the (Feigenbaum) period-doubling cascade occurs in difference equations [1], differential equations [2] and fluid experiments [3]. The phenomenon of intermittency [4] has also been widely observed in the above types of system [5], which argues persuasively that it is a "universal" kind of behaviour. To a lesser extent, hysteresis (representing the concurrent existence of different stable trajectories in dynamical systems) is also commonly observed [6], and indeed might be expected in any system which can behave intermittently: for example, the Rössler equations exhibit hysteresis, period-doubling, and intermittency in various ranges of their parameter space [7].

2. The best-known dynamical system, the Lorenz equations $\dot{X} = -\sigma X + \sigma Y$, $\dot{Y} = (r - Z)X - Y$, $\dot{Z} = XY - bZ$, is known to exhibit period-doubling [8] and intermittency [9], and one might reasonably expect hysteresis as well; indeed, it is well-known [10] that for the "standard" values $\sigma = 10$, $b = 8/3$, the non-trivial fixed points ($Z = r - 1$, ...) coexist (stably) with the strange attractor for $24.06 \lesssim r \lesssim 24.74$, and hence hysteresis occurs in this range: for higher r, transitions can be intermittent.

All these phenomena, and particularly hysteresis, can be explained on the basis of a suitable non-monotone difference equation [11], such as that relating successive maxima of Z constructed by Lorenz [12], which exhibits a pronounced cusp. In turn, this can be readily understood as being due to the occurrence of a homoclinic orbit in the system [13]: as r passes through the value at which the homoclinic "explosion" takes place, a strange invariant set of trajectories is produced, including an infinite number of periodic orbits [14,15]. It may be better to think of period-doubling windows as being a result of the existence of homoclinicity in a system (which "produces" the orbits which are then "absorbed" by the period-doubling window) rather than as being primarily due to successive bifurcations of a parent periodic orbit. This view is derived from that of Sparrow, as expressed in his forthcoming book [15].

3. The "Lorenz map" relating successive maxima of Z on the strange attractor should be a curve crossed with a Cantor set; that Lorenz observed a single-valued function is directly due to the strong contraction rate of phase volumes. In turn, this can be considered as being due to the large value of σ in his computation. We have taken advantage of this observation to con-

0 031-9163/82/0000–0000/$02.75 © 1982 North-Holland

struct a Lorenz map *analytically* when σ and r are both large. The construction uses the technique of singular perturbation analysis as applied to relaxation-type oscillations [16]. Specifically we define $\rho = r/\sigma$, $\delta = b/\sigma$, and analyse the equations in the limit $\rho \sim O(1)$, $\delta \ll 1$; at leading order one obtains a complicated difference equation relating M_{n+1} to M_n, where rM_n is the nth maximum of Z on a trajectory: in its simplest form (and for $|M_n - (1 + 1/4\rho)| \ll 1$) this difference equation can be written parametrically as

$$M_n = (1 + 1/4\rho)\left[1 + \frac{\delta^{2/3}2^{2/3}\zeta}{(1 + 4\rho)^{1/3}}\right],$$

$$M_{n+1} = 2 - k|Ai(-\zeta)|^{\beta} \exp(-\lambda\delta^{2/3}\zeta), \qquad (1)$$

where

$$k = 4(1 + 1/4\rho)\exp\{-2[(1 + 4\rho)^{1/2} - \ln 2] \times [(1 + 4\rho)^{1/2} - 1]^{-1}\},$$

$$\beta = 2\delta/[(1 + 4\rho)^{1/2} - 1],$$

$$\lambda = 2^{2/3}/\{(1 + 4\rho)^{1/3}[(1 + 4\rho)^{1/2} - 1]\}.$$

The form of this difference equation is shown in fig. 1; as also found by Lorenz [17] for decreasing b (so also $\delta \to 0$), there are multiple cusps superimposed on a cuspless "envelope" curve; these are of "thickness' $\exp[-O(1/\delta)]$, and spaced $O(\delta^{2/3})$ apart.

Fig. 2 shows the result of a numerical solution of the equations. All the interesting dynamic transitions occur when a cusp approximately overlies the intersection of the 45° line with the envelope curve. This happens at a sequence of values $\rho = \rho_s$, $s = 1, 2, \ldots$ when the first, second, etc. cusp overlies the fixed point of the envelope curve, at a sequence of values $M_n = C_s$. The values ρ_s (and also C_s) are $O(\delta^{2/3})$ apart, and interesting behaviour is when $|\rho - \rho_s| = O(\delta)$ (otherwise the difference equation has a simple fixed point, corresponding to a periodic solution of the Lorenz system). Putting $M_n = C_s + \delta\mu_n$, $M_{n+1} = C_s + \delta\mu_{n+1}$, $\rho = \rho_s + \delta\chi\tilde{\rho}$, where χ is an O(1) constant, one derives the locally approximate *canonical difference equation*

$$\mu_{n+1} = \tilde{\rho} + \kappa(\mu_n - \Omega \ln|\mu_n|), \qquad (2)$$

where κ, Ω are O(1) constants. To the same order of approximation given by (1),

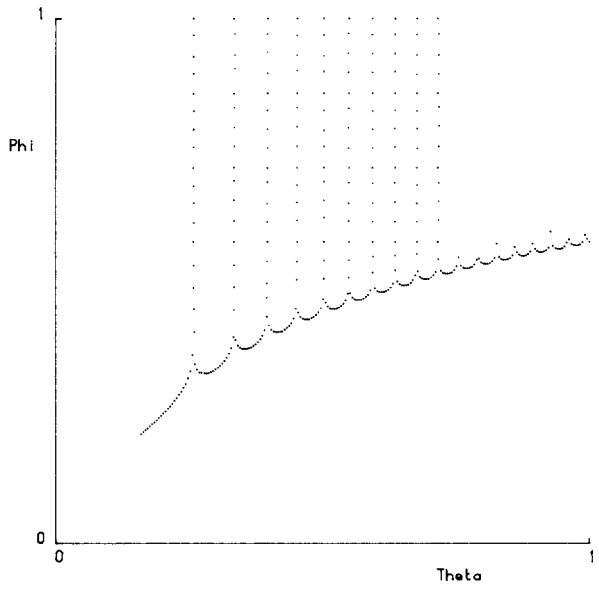

Fig. 1. Form of the difference equation from a slightly more accurate version of (1), at parameter values $\sigma = 100$, $r = 160$, $b = 1$: the first ten cusps have been indicated. Here $M_n = 1 + \theta$, $M_{n+1} = 1 + \phi$.

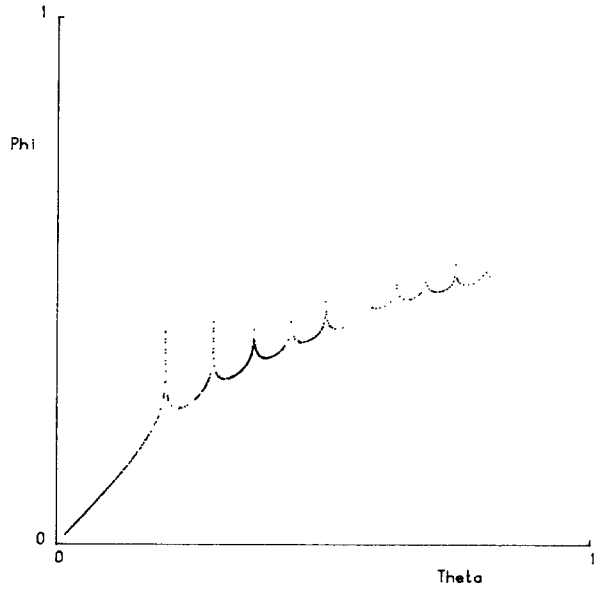

Fig. 2. Difference map obtained from a direct numerical integration of the Lorenz equations at the same parameter values as fig. 1. The full height of the cusps is not seen because of their narrowness. There are obvious quantitative discrepancies, but we wish to point out the *qualitative* similarity.

$$\kappa = \frac{2^{4/3}\rho\lambda k}{(1+4\rho)^{2/3}}, \quad \Omega = 2^{1/3}(1+4\rho)^{1/3}, \qquad (3)$$

evaluated at $\rho = \rho_s$. (The invalidity of (2) when $\mu_{n+1} \gg 1$ does not materially affect the dynamics.)

4. The derivation of the Lorenz map is carried out in detail elsewhere [18], as is the derivation and analysis of (2) [19]. Here we sketch some typical results. We call the trough between the sth cusp and the $(s+1)$th cusp the sth trough, T_s. For each cusp number, we identify the corresponding $r_s = \sigma\rho_s$ for which the cusp overlies the fixed point of the envelope equation. Generally $\{r_s\}$ is an increasing sequence. For *each* value of s, there is a value $r_s^{(1)}$ such that for $r < r_s^{(1)}$, there is a stable T_{s-1} fixed point (and an unstable one); at $r_s^{(1)}$ these coalesce (a saddle-node bifurcation), and if $\kappa < 0.2178...$ the resultant motion is "probably" chaotic (in T_s). (This stems from the fact that when the relation $\mu_{n+1} = f(\mu_n)$ given by (2) has two coalescent fixed points, let us say $\mu = \mu_c$, it turns out that the minimum value of f for $\mu > 0$ [at $\mu = \Omega$, i.e. $f_{\min} = \tilde{\rho} + \kappa\Omega(1 - \ln\Omega)$] is greater or less than μ_c depending on whether $1/(1-\kappa) + \ln[\kappa/(1-\kappa)]$ is greater or less than 0, and these correspond to κ being greater or less than $\zeta/(1+\zeta)$, where $\zeta e^{\zeta} = e^{-1}$, i.e. κ greater or less than 0.2178... . If κ is greater than 0.2178..., then the minimum of f in $\mu > 0$ is greater than the value of f at μ_c, and so when the saddle-node bifurcation takes place, trajectories move towards $\mu > 0$, in which region they then remain.)

On the other hand, for sufficiently high r (but near r_s), there is a stable T_s fixed point; this becomes unstable (to a two-cycle) as r decreases through $r_s^{(3)}$. For $\kappa < 0.2178... r_s^{(3)} > r_s^{(1)}$, and as r decreases below $r_s^{(3)}$, a period-doubling window ensues. However, if $\kappa > 0.2178..$, then $r_s^{(1)} > r_s^{(3)}$, and for $r_s^{(1)} > r > r_s^{(3)}$, there exist concurrent fixed points (i.e. periodic orbits of the differential equations). As r decreases below $r_s^{(3)}$, a period-doubling route towards chaos ensues; at a lower value $r_s^{(4)}$, stable aperiodic motion visits T_{s-1} *and* T_s; finally, at a value $r_s^{(2)}$ (if $\kappa > 0.2178...$) (when the chaotic T_s trajectory includes the stable manifold of the unstable T_{s-1} fixed point), the T_s motion becomes unstable, and the T_{s-1} stable fixed point is (almost) globally attracting. Consequently, when $\kappa > 0.2178...$ there is an interval $r_s^{(2)} < r < r_s^{(1)}$ in which two different stable (non-constant) solution behaviour are possible, and transition between them is hysteretic.

Table 1
Values of $r_s^{(i)}$ for $\sigma = 300$, $b = 1$; κ is 0.68 and 0.63 for $s = 1$, 2 respectively.

s	$r_s^{(1)}$	$r_s^{(2)}$	$r_s^{(3)}$	$r_s^{(4)}$
2	240.5	223.6	233.6	229.4
3	271.5	252.6	266.5	261.1

Computation of κ shows that κ increases with σ, so it is plausible to expect intermittency to occur for lower σ, hysteresis for high σ. The expression for κ in (3) does not reveal a dependence on σ (at fixed ρ), but one can perhaps see from (1) that a more accurate expression for κ will reveal such a dependence. More obviously, κ is the (local) slope of the envelope curve [e.g. compare κ in (3) with dM_{n+1}/dM_n in (1)], and increasing κ with σ simply indicates that this envelope becomes "steeper" as σ increases: or, in terms of figs. 1 and 2, the troughs become shallower as σ increases; this, incidentally, is in accord with Lorenz's map, where only the first trough is observed at $\sigma = 10$.

The range of r over which transition occurs is $\sigma \times O(\delta) = O(1)$; however, due to various factors of "order unity" which are actually quite substantial, the numerical range is somewhat larger than this. For example, table 1 shows values $r_s^{(i)}$ for $s = 2, 3$ at $\sigma = 300$, $b = 1$. On the basis of these, we would predict the results shown in table 2, which also shows results taken from a direct numerical solution of the equa-

Table 2
Comparison of predicted and observed behaviour for $\sigma = 300$, $b = 1$. Here f.p. = fixed point, ap.m. = aperiodic motion, p.d.w. = period-doubling window.

Predicted		Observed
$r < 223.6$	T_1 f.p.	220, 225
$223.6 \rightarrow 229.4$	T_1 f.p. $T_{1,2}$ ap.m.	230
$229.4 \rightarrow 233.6$	T_1 f.p. T_2 p.d.w.	239 (T_2 two-cycle)
$233.6 \rightarrow 240.5$	T_1 f.p. T_2 f.p.	240, 246
$r < 252.6$	T_2 f.p.	250
$252.6 \rightarrow 261.1$	T_2 f.p. $T_{2,3}$ ap.m.	260
$261.1 \rightarrow 266.5$	T_2 f.p. T_3 p.d.w.	270 (T_3 two-cycle)
$266.5 \rightarrow 271.5$	T_2 f.p. T_3 f.p.	unavailable
$r < 287.0$ ($=r_4^{(2)}$)	T_3 f.p.	280

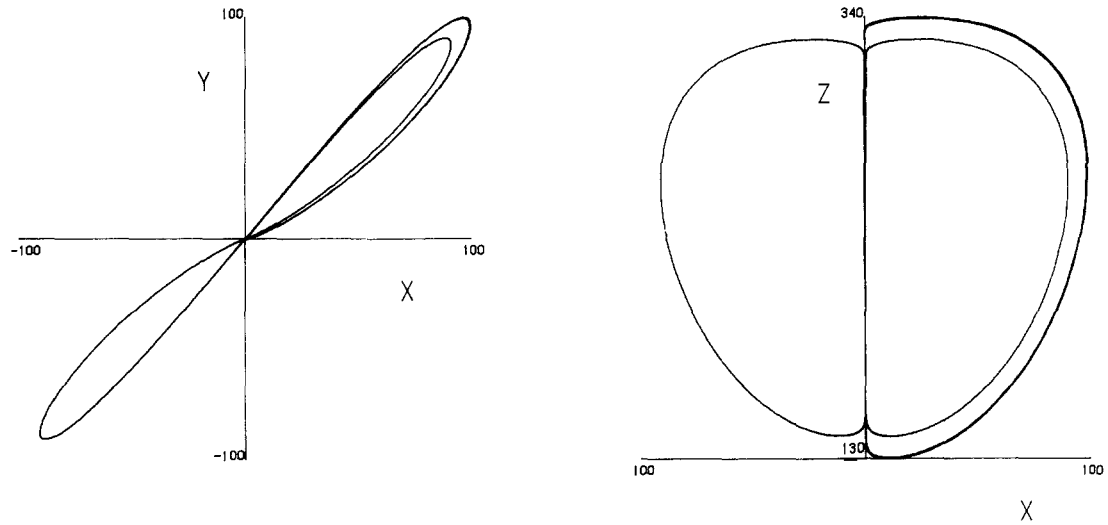

Fig. 3. Phase plots of stable T_1 and T_2 limit cycles at $r = 240$, $\sigma = 300$, $b = 1$. The inner (T_1) cycle has one crossing of $X = 0$ between maxima of Z, and hence gives the apple-shaped curve on the X–Z plot. The other (T_2) has two crossings, so that X, Y are (mostly) one-signed. It has a symmetrical counterpart with X, $Y < 0$. Note the close approach of both limit cycles to the Z-axis.

tions. The bifurcation sequence is correctly predicted, and the numerical values of the transition parameters are fairly accurate. Fig. 3 shows phase plots of the stable T_1 and T_2 limit cycles (fixed points) at $r = 240$, $\sigma = 300$, $b = 1$. Note that at these values of σ and b, the non-trivial fixed points ($M_n \approx 1$) are linearly stable until $r = \sigma(\sigma + b + 3)/(\sigma - b - 1) \approx 306$, so that at $r = 240$ (for example) we have two stable limit cycles *and* a stable fixed point: two hysteresis bands overlap.

References

[1] R.M. May, Nature 261 (1976) 459.
[2] V. Franceschini and C. Tebaldi, J. Stat. Phys. 21 (1979) 707.
[3] A. Libchaber, C. Laroche and S. Fauve, J. Phys. Lett. 43 (1982) L211.
[4] P. Manneville and Y. Pomeau, Physica 1D (1980) 219.
[5] G. Mayer-Kress and H. Haken, Phys. Lett. 82A (1981) 151;
J. Maurer and A. Libchaber, J. Phys. Lett. 41 (1980) L515;
S. Fraser and R. Kapral, Phys. Rev. 23A (1981) 3303.
[6] E. Ott, Rev. Mod. Phys. 53 (1981) 655;
J. Maurer and A. Libchaber, J. Phys. Lett. 40 (1979) L419.
[7] S. Fraser and R. Kapral, Phys. Rev. A25 (1982) 3223.
[8] K.A. Robbins, SIAM J. Appl. Math. 36 (1979) 457.
[9] P. Manneville and Y. Pomeau, Phys. Lett. 75A (1979) 1.
[10] J.A. Yorke and E.D. Yorke, J. Stat. Phys. 21 (1979) 263.
[11] C. Tresser, P. Coullet and A. Arneodo, J. Phys. Lett. 41 (1980) L243.
[12] E.N. Lorenz, J. Atmos. Sci. 20 (1963) 130.
[13] K.A. Robbins, Math. Proc. Cambridge Phil. Soc. 82 (1977) 309.
[14] J. Guckenheimer, in: The Hopf bifurcation and its applications, eds. J.E. Marsden and M.J. McCracken (Springer, Berlin, 1976) p. 368.
[15] C. Sparrow, Bifurcations in the Lorenz equations (Springer, Berlin), to be published.
[16] J. Kevorkian and J.D. Cole, Perturbation methods in applied mathematics (Springer, Berlin, 1981).
[17] E.N. Lorenz, in: Global analysis, eds. M. Grmela and J.E. Marsden (Springer, Berlin, 1979) pp. 53–75.
[18] A.C. Fowler and M.J. McGuinness, Physica D (1982), to be published.
[19] A.C. Fowler and M.J. McGuinness, Stud. Appl. Math., to be published.